VOLVO

DE-FC26-05NT42417

Demonstration of Air-Power-Assist Engine Technology for Clean Combustion and Direct Energy Recovery in Heavy Duty Application

Final Report

13 March 2008

Hyungsuk Kang, Ph.D
Volvo Powertrain North America
13302 Pennsylvania Avenue
Hagerstown, MD 21742
301-790-5400 ext 5388
hyungsuk.kang@volvo.com

Chun Tai, Ph.D
Group Leader, Advanced Combustion
Volvo Powertrain North America
13302 Pennsylvania Avenue
Hagerstown, MD 21742

Samuel Taylor
Program Manager
National Energy Technology Laboratory
3610 Collins Ferry Road, P. O. Box 880
Morgantown, WV 26507-0880

Project SUMMARY

During the fourth quarter of Phase III from October to December 2007, the final Air-Power-Assist (APA) engine testing was completed and a final review meeting with DOE agents was held on Nov. 29th 2007 at VPTNA, Hagerstown, MD.

The APA project was initiated from September 2005 to January 2008. The following is the summary of each Phase.

Phase I (09/01/05 – 12/31/05)

The first phase of the project consists of four months of applied research, starting from September 1, 2005 and was completed by December 31, 2005. During this time, the project team heavily relied on highly detailed numerical modeling techniques to evaluate the feasibility of the APA technology. Specifically,

- A GT-Power™ engine simulation model was constructed to predict engine efficiency at various operating conditions. Efficiency was defined based on the second-law thermodynamic availability.
- The engine efficiency map generated by the engine simulation was then fed into a simplified vehicle model, which was constructed in the Matlab/Simulink environment, to predict fuel consumption of a refuse truck on a simple collection cycle.
- Design and analysis work supporting the concept of retrofitting an existing Sturman Industries Hydraulic Valve Actuation (HVA) system with the modifications that are required to run the HVA system with Air Power Assist functionality. A Matlab/Simulink model was used to calculate the dynamic response of the HVA system. Computer aided design (CAD) was done in Solidworks for mechanical design and hydraulic layout.

At the end of Phase I, 11% fuel economy improvement was predicted.

Phase II (01/01/06 – 10/31/06)

During Phase II, the engine simulation group completed the engine mapping work. The air handling group made substantial progress in identifying suppliers and conducting 3D modelling design. Sturman Industries completed design modification of the HVA system, which was reviewed and accepted by Volvo Powertrain.

In Phase II, the possibility of 15% fuel economy improvement was shown with new EGR cooler design by reducing EGR cooler outlet temperature with APA engine technology from Air Handling Group. In addition, Vehicle Simulation with APA technology estimated 4 -21% fuel economy improvement over a wide range of driving cycles.

Phase III (02/01/07 – 01/31/08)

During Phase III, the engine experimental setup was initiated at VPTNA, Hagerstown, MD. Air Handling system and HVA system were delivered to VPTNA and then assembly of APA engine was completed by June 2007.

Functional testing of APA engine was performed and AC and AM modes testing were completed by October 2007. After completing testing, data analysis and post processing were performed. Especially, the models were instrumental in identifying some of the key issues with the experimental HVA system.

Based upon the available engine test results during AC and AM modes, the projected fuel economy improvement over the NY composite cycle is 14.7%. This is close to but slightly lower than the originally estimated 18% from ADVISOR simulation.

Project Summary

The APA project group demonstrated the concept of APA technology by using simulation and experimental testing. However, there are still exists of technical challenges to meet the original expectation of APA technology. The enabling technology of this concept, i.e. a fully flexible valve actuation system that can handle high back pressure from the exhaust manifold is identified as one of the major technical challenges for realizing the APA concept.

Content

1 Design Analysis, Diagnostic and Fundamental Studies Using Single and Multicylinder Simulation of the ICE/Pneumatic Engine System Summary

1.1 Introduction and Review of APA (Pneumatic Hybrid) System Model

Reports for prior phases of the program have detailed specific applications of the system models used in the APA program. This report will add documentation of analyses carried out during Phase III. As this Phase involved preparation for and dynamometer testing of the APA system, most of the analytical work is focused on studies to assist in developing various components of the experimental system, operational procedures and, ultimately, diagnostic work related to the experimental results obtained.

Prior to a description of the Phase III analytical studies, it is appropriate in this final Phase III report to provide a comprehensive review of the system models employed.

The Air Power Assisted (APA) Engine System Model, created using the GT- Power™ commercial engine software package, is a highly detailed and flexible simulation model that whose purpose is to assist with the optimization of the design, operation and control of pneumatic (air) hybrid propulsion systems. It simulates the propulsion and air storage system in all modes – ICE, Air Compressor (AC) and Air Motor (AM) – in steady-state, transient and transitional operation.

The code was originally developed between 2002-2004 for a light duty pneumatic hybrid project (5.4L V-8 in Ford F150) sponsored by Social Profit Network, Inc. (SPN) of Menlo Park, CA. SPN is a not-for-profit corporation that sponsors R&D in areas that are beneficial to society. The 5.4L V-8 ICE model was validated with experimental data. The code was licensed on a non-exclusive basis to Volvo Group AB for use in the DOE Air Power Assist program in order to get a quick start on the analytical effort.

Subsequent to the start of the DOE/Mack/VPT program, the Ford V-8 spark-ignited ICE model was replaced by an existing Mack MD11 diesel engine model. The Pneumatic System Submodel was enhanced, especially with respect to a more fundamental and useful definition of efficiency in hybrid modes. The Thermodynamic Availability of the Air Tank contents is computed at all instants of time in order to track the maximum work extractable with respect to ambient “sink” conditions. In addition, valve lift and valve timing definitions were modified to conform to Sturman Industries Hydraulic Valve Actuator (HVA) conventions.

For simulations not requiring the complexity of the full multicylinder model such as the presence of the turbocharger and intercooler, a special single cylinder version was developed, allowing for more detailed studies of phenomena related to efficiency, valve timing, lift profiles and the like. Comparisons were carried out between the results produced by the single cylinder (SC) and multicylinder models (MC) to ensure proper implementation and that the results agreed in fundamental respects.

The next three subsections describe the key capabilities and submodels of the overall simulation corresponding to the major submodels of the simulation:

- Reciprocating Engine
- Pneumatic (Air) System Submodel (PSS)

- Cylinder Activation, Fueling and Valve Control (CAFVC)

1.1.1 Reciprocating Engine Submodel (Operating Modes: ICE, AC, AM)

The reciprocating engine submodel of the Mack MD11 engine was developed by Mack/Volvo Powertrain (VPT). It is a state-of-the-art GT-Power™ model of the MD11, six cylinder, turbocharged, and intercooled diesel engine. It contains all the features that would normally be expected in a comprehensive diesel engine model.

The SC submodel was abstracted from the MD11 MC submodel with all critical cylinder, inlet and outlet flow dimensions intact in order to explore conceptual issues without the complexity of multicylinder interactions. It also simplifies the development of additional features in other submodels without the computational requirements of the full MC model. A picture of the SC version of the GT-Power "project map" – i.e., the GUI of the model – absent turbocharger and intercooler systems is shown in Figure 1.1.1.1.

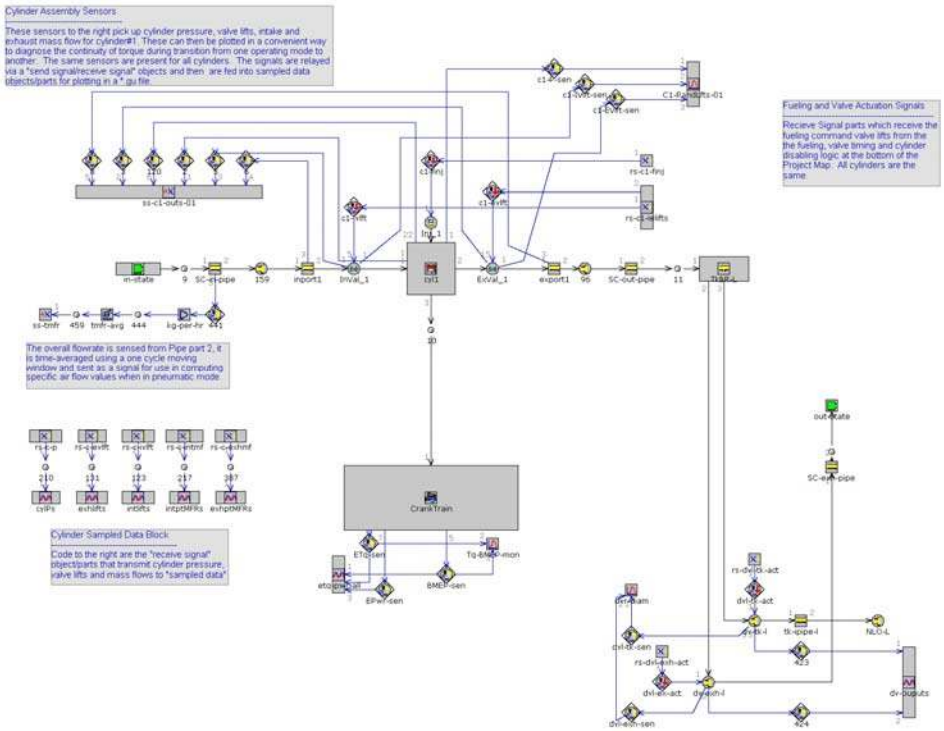

Figure 1.1.1.1. Single Cylinder Version of MD11 Reciprocating Engine Submodel Showing 3-Way Diverter Valve (lower right).

At the lower right of Figure 1.1.1.1, a 3-Way Diverter Valve (DV) assembly has been added which enables switching the flow from the traditional ICE exhaust system to the air storage system during pneumatic modes of operation and vice versa. The representation is fully flexible in that any time-based function can be used to represent the opening and closing of the two parts of the valve assembly, including a time delay between the valve which is actuated first and the second valve of the assembly. In addition, the DV can be actuated at any specific cycle in the simulation, with a specifiable crank angle degree delay from the start of the cycle. This is an important capability when there is need to run simulations which incorporate transitions between modes of operation, e.g., the most common being

ICE to AC or AM to ICE. The 3-Way DV assembly, or something equivalent, is a requirement that is specific to APA propulsion systems.

1.1.2 APA Pneumatic System Submodel (Operating Modes: AC, AM)

The Pneumatic System Submodel (PSS) is a unique submodel created especially for pneumatic hybrid or, APA, systems. Figure 1.1.2.1 shows a section of GT-Power project map of the PSS.

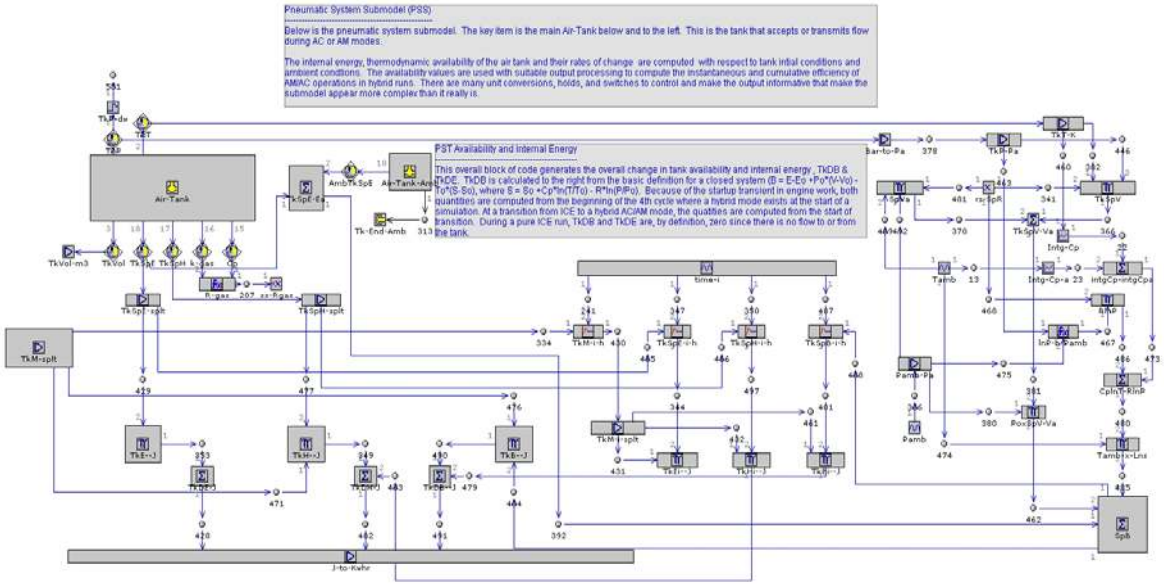

Figure 1.1.2.1 Major Section of PSS showing Air Tank and Computational Tracking of Enthalpy, Internal Energy, Entropy and Thermodynamic Availability.

The PSS provides a complete description of the contents of the Air Tank by tracking, at each instant of time, the pressure (P), temperature (T), specific values of enthalpy (H), internal energy (E), entropy (S) and thermodynamic availability (B) of the contents of the tank. The mass of air in the tank is computed from the inflows and outflows, also on an instantaneous basis. Although the full link is not shown due to space limitations, when the DV of Figure 2.1 is configured in APA mode, the flow between the Air Tank and the (non-fueled) Reciprocating Engine is enabled through the flow path at the upper left of Figure 1.1.2.1.

The work function referred to as “Thermodynamic Availability” or availability was added to the PSS during the Phase I work to obtain a measure of the true efficiency of pneumatic mode operation. The internal energy of the Air Tank is not sufficient since it can be in the form of higher temperature and lower pressure which has less work potential than a tank of equivalent internal energy at lower temperature and higher pressure into the Air Tank if all work were accomplished through a Carnot engine, with the ambient, denoted by “o”, serving as the low temperature sink.

The change in the specific availability of the air contents of the tank with respect to the ambient, ΔB, is given by the equation for a "closed system"

$$\Delta B = E - Eo + [Po \times (V - Vo)] - To \times (S - So)$$

In the actual implementation, the entropy, S, is computed from the expression

$$S - So = \int Cp \times dT/T - R \times \ln (P/Po)$$

where the integral is evaluated between To and T. Since Cp for air varies with temperature over the range of interest, this integral has been pre-computed from a special form of the code and is stored in a look-up table vs. temperature, T. From a theoretical point of view, the availability, B, represents the maximum work that can be extracted or put into the Air Tank if all work were accomplished through a Carnot engine, with the ambient, denoted by "o", serving as the low temperature sink.

The rate of change of availability compared with the engine power (either with or without engine friction) provides values of the instantaneous "indicated" or "brake" efficiencies in AC and AM modes. The values are the best equivalent to the usual definitions of thermal efficiency in ICEs. The pneumatic efficiencies are given by the following expressions:

Air Compressor (AC)

$$\text{Efficiency (Ind./Brake)} = - \frac{\text{Rate of Change of Availability}}{\text{Engine Power (Ind./Brake)}}$$

Air Motor (AM)

$$\text{Efficiency (Ind./Brake)} = - \frac{\text{Engine Power (Ind./Brake)}}{\text{Rate of Change of Availability}}$$

Much of the remainder of the PSS, which is not shown in Figure 1.1.2.1, is concerned with calculating the efficiencies from the basic quantities and other important variables such as specific airflow and rate of change of Air Tank mass. Also, there is complex logic to control the output of these quantities in a meaningful way when operating in pneumatic (air hybrid) modes or in transitional operation between pneumatic and ICE modes.

1.1.3 Cylinder Activation, Fueling and Valve Control - CAFVC - (Operating Modes: ICE, AC, AM)

This subsystem module referred to as CAFVC is critical to simulating an APA propulsion system. It provides complete and separate control as to which cylinders will be active with respect to valve motion and fueling. In other words, cylinders can be completely deactivated or simply not fueled in any cycle sequence desired by the user of the simulation.

The CAFVC also allows easy specification of different theoretical valve profiles such as ramps or multi-rate ramps. This is critical to the effort as Sturman Industries was in the process of developing the HVA in the earlier phases of the program and various projected alternatives required continuous evaluation. With minor modifications, actual experimental valve profile vs. crank angle traces can also be implemented as seen in later sections 1.2.9 and 1.2.10 that deal with analysis of the experimental results.

In specific, this module provides the following flexibilities and capabilities:

- Within one 720 degree cycle, either 1 or 2 intake and exhaust events and ability to program transition between 2-stroke and 4-stroke operation as a function of cycle number.
- "Master valve objects" to define any set of lift profiles for each cycle sequentially or specially constructed input lifts for detailed study of transition between modes within a single cycle.
- Within one 720 cycle, ability to separately specify cylinder- by-cylinder fueling and valve actuation.
- Separate time multipliers for intake and exhaust valve opening and closing events.
- Separate lift multipliers for intake and exhaust valves.

The CAFVC module is essentially a representation of a very flexible "camless" valve system.

A meaningful copy of either the entire CAFVC "project map" – or a part thereof – cannot be provided in the format of this report due its integrated nature, its size and complexity.

1.2 Design Analysis and Diagnostic Studies – Phase III

As indicated in the Introduction, most of the analytical work in Phase III was focused on studies to assist in developing various components of the experimental system, operational procedures and diagnostic work related to the experimental results obtained. These studies are described below.

1.2.1 Effect of Exhaust Manifold Diameter on AC Efficiency at 6 bar Air Tank Pressure and at 1800, 1200 and 600 RPM

Earlier studies had indicated that the ~45 mm exhaust manifold diameter (runners and logs) posed a restriction to air flow under conditions of high gas velocity, i.e., low Air Tank pressure and high engine speed. A recommendation for a 60 mm exhaust manifold had been made. Due to considerations related to mechanical and thermal stress, the VPT Air Handling team could not achieve 60 mm but was working toward an approximately 55 mm diameter design.

Therefore, it was determined to repeat the earlier simulations over a range of exhaust manifold diameters from 45 mm to 60 mm at various engine speeds to determine the effect, if any, of reducing the diameter. The latest values of piping diameters/lengths and 3-way valve diameters were used in the study.

Typical valve timings near optimal for Air Compression (AC) mode were chosen for the study. Figure 1.2.1.1 shows the valve lift profiles at 1800 RPM.

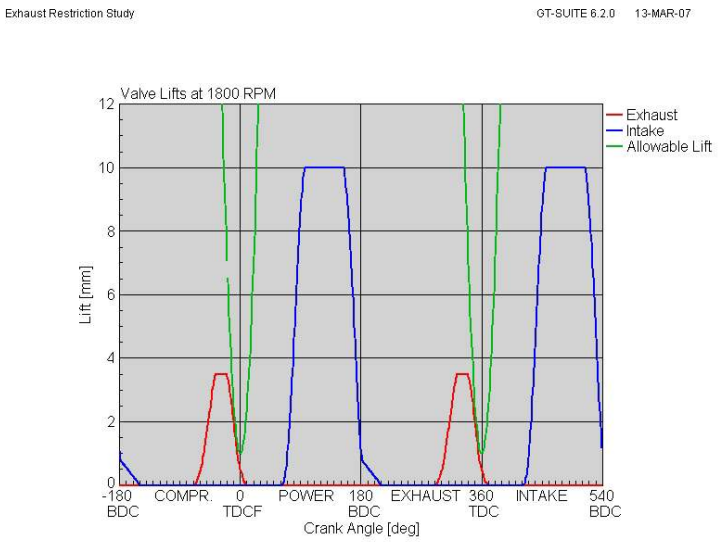

Figure 1.2.1.1. Valve Lifts and Clearance (Allowable Lift) at 1800 RPM

The same valve timings were used at 1200 and 600 RPM even though the clearance requirement was not maintained. In studying the effect of exhaust manifold restriction, 1800 RPM would be the most severe case and the clearance violation would have no effect on predicting the trends vs. exhaust manifold diameter at lower engine speeds.

Contrary to previous results, it was found that between 45 mm and 60 mm the exhaust manifold inner diameter had little effect on the indicated efficiency, as shown in Figure 1.2.1.2. On the expanded scale of the plot, it can be said that the efficiency is insensitive to diameter over the range studied. The efficiency increases with decreasing engine speed since closer to isentropic engine cycles can be achieved due to lower pressure losses overall. This will be evident from P-V diagrams (Figure 1.2.1.5) to be shown later.

Considerable effort was spent to understand why previous simulations identified the exhaust manifold diameter as a significant restriction and the current simulation did not. The three-way valve diameter was increased, the pipe diameter to the Air Tank was increased, the length of the pipe decreased to see if these variables posed the more significant restriction. The results were negative and the efficiency remained flat as a function of exhaust manifold diameter. The only significant change that had been introduced (other than the above dimensions) was the insulation of the exhaust manifold. In the prior simulations, the exhaust manifold was not thermally insulated, allowing heat transfer between the manifold walls and the gas. The wall temperature had been set at ~850 deg K. Therefore, at larger diameters, the effect was to allow more time for thermal energy from the exhaust manifold to enter the airflow, thereby indicating a higher efficiency. With the manifold insulated, this effect was removed and efficiency was not affected by manifold wall temperature.

In the real system, AC will typically follow ICE operation and the manifold walls will be hot. However, if the manifold is insulated this heat will drawn out of the metal manifold quickly. Therefore, the new results are considered more reliable, even if not an exact reproduction of realistic transient operation.

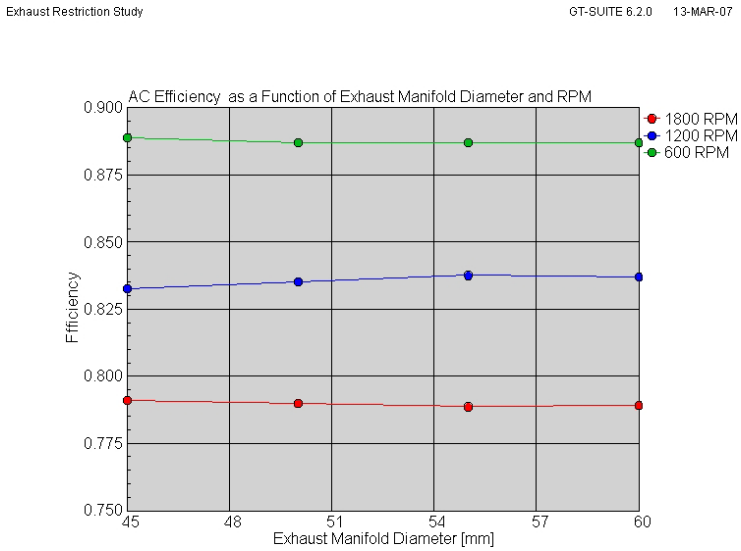

Figure 1.2.1.2. Indicated Efficiency vs. Exhaust Manifold Inner Diameter at 1800, 1200 and 600 RPM.

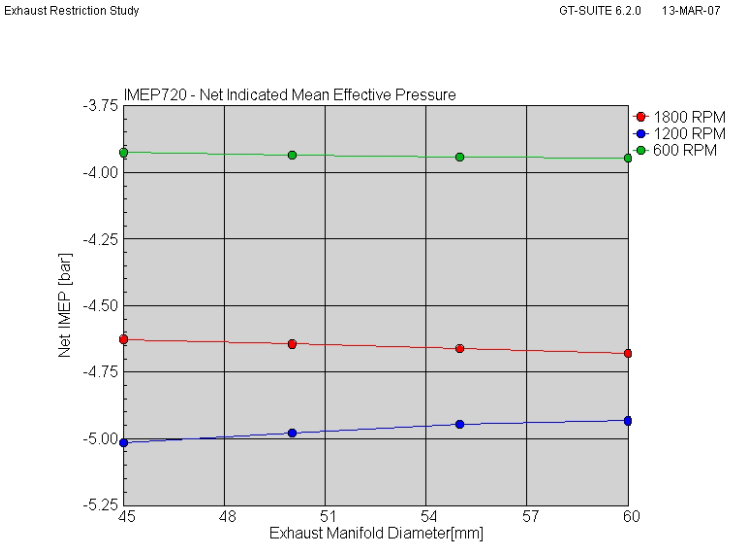

Figure 1.2.1.3. IMEP vs. Exhaust Manifold Inner Diameter at 1800, 1200 and 600 RPM.

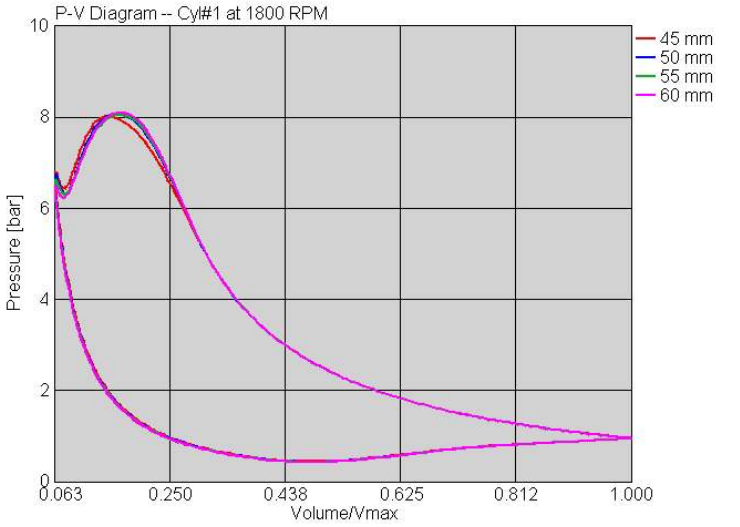

Figure 1.2.1.4. P-V Diagrams at 1800 RPM as a Function of Exhaust Manifold Inner Diameter.

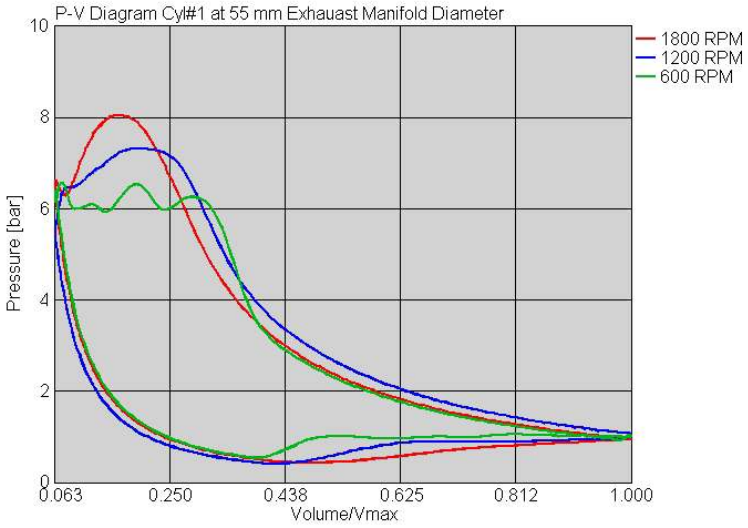

Figure 1.2.1.5. P-V Diagrams at 55 mm Exhaust Manifold Inner Diameter as a Function of Engine Speed.

1.2.2 Effect of Mass Flow Meter Diameter on Efficiency During AC Operation at 2100 RPM/6 bar Air Tank Pressure – "Worst Case Conditions"

In preparation for studies involving the experimental system to be installed at Volvo Powertrain, the multicylinder model was upgraded to reflect the new exhaust manifold design, the exhaust-side 3-way valve and the piping configuration to the air tank. The modeling of the exhaust manifold is more complex then is typical due to the varying diameter of the manifold log and the large center opening and flange which connect to the 3-way valve. Gamma Technologies Inc, the supplier of GT-Power software, was consulted on the most appropriate technique. Note that the final model of the exhaust manifold and air pipe-to-Air Tank system that was developed during the APA program would still require upgrading to capture thermal transients and to correctly solve for wall temperatures, using the dimensions and characteristics of the system components and actual insulating materials.

At the request of the Volvo Air Handling group, a specific study was carried out to help support the choice of an appropriate mass flow meter (MFM) to be used to determine the flow rate to the Air Tank, an important experimental parameter. The meter was assumed to be six inches in length (152.4 mm) and of varying possible diameters ranging from 1 inch to 3 inches. It was placed in the center of the 3 ft (914.4 mm) section of air tank piping, connected to it with converging and expanding sections of pipe whose length was maintained constant at 3 inches and whose larger diameter was 3 inches (76.2 mm). The diameter of the MFM was varies in 4 equal increments between the minimum value of 1 inch and 3 inches. The total number of cases studied was 5; diameters were 25.4, 38.1, 50.8, 63.5 and 76.2 mm. It was assumed that there was no further obstruction of the flow within the MFM.

The valve timing conditions, which give results close to "equilibrium", are shown in Figure 1.2.2.1 along with the resulting P-V diagrams in Figure 1.2.2.2.

INTENTIONALLY LEFT BLANK

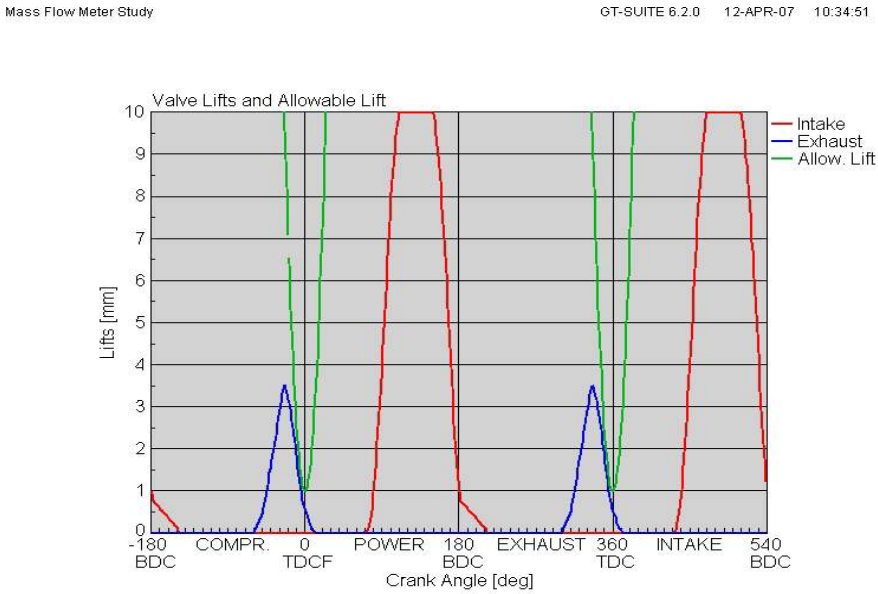

Figure 1.2.2.1. Valve Lifts and Allowable Clearance Line

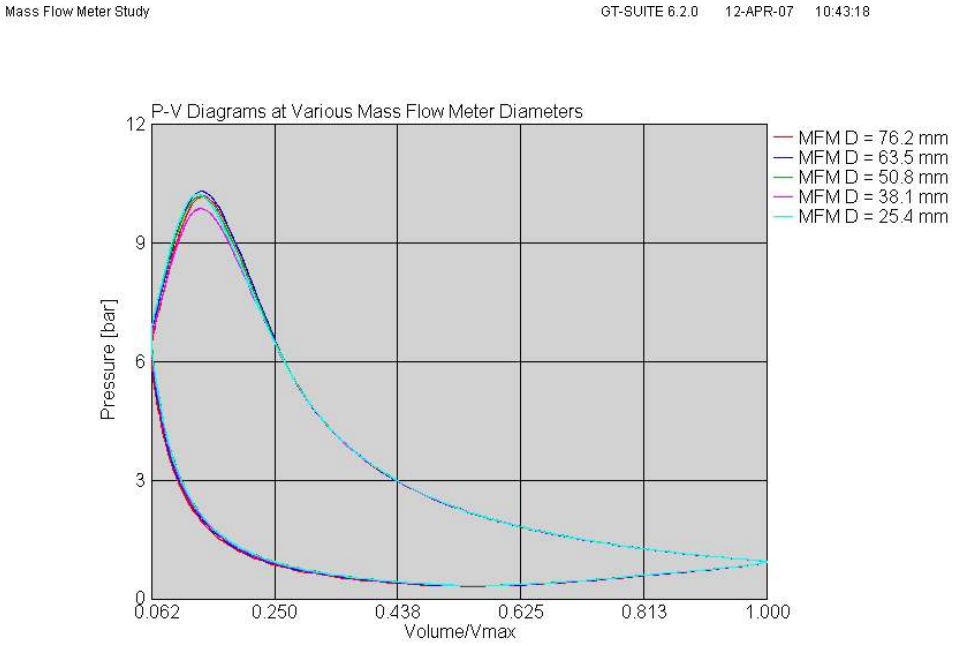

Figure 1.2.2.2. P-V diagrams for the Different MFM Diameters Simulated

The P-V diagrams (as well as the rest of the data to be shown later) do not exhibit a monotonic trend vs. MFM diameter. This can be due either to numerical dispersion effects of the dicretization or to gas dynamic effects. Since the net result of the study showed that the choice of MFM diameter -- within the range studied -- had little effect on AC efficiency, IMEP, pressure drop across the MFM or airflow, the slight dispersion of results was not

investigated further. The most plausible explanation is that the dominant cause of the dispersion is due to gas dynamic effects resulting from cylinder pulsations.

Figures 1.5.1.3, 1.5.1.4, and 1.5.1.5 show the AC Efficiency, IMEP and specific airflow as a function of MFM diameter. Although not shown the pressure drop across the MFM was negligible for all MFM diameters studied.

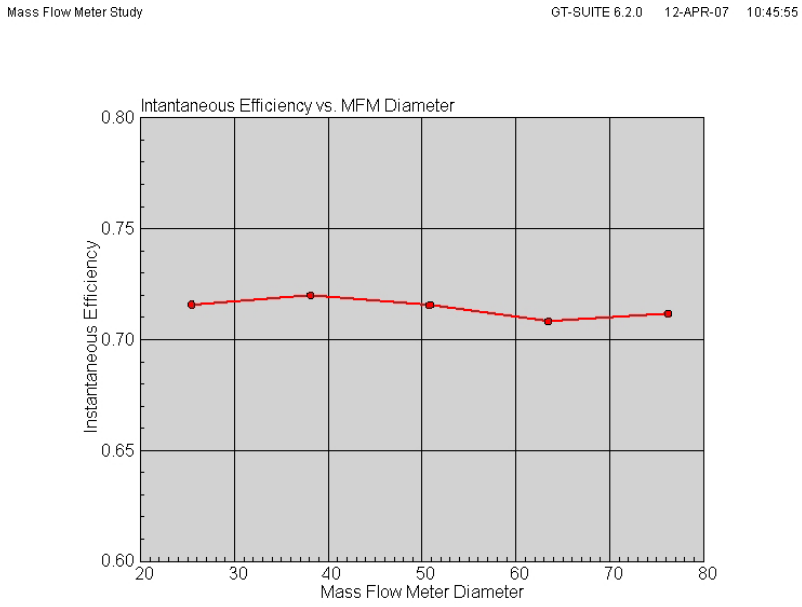

Figure 1.2.2.3. AC Efficiency vs. MFM Diameter

INTENTIONALLY LEFT BLANK

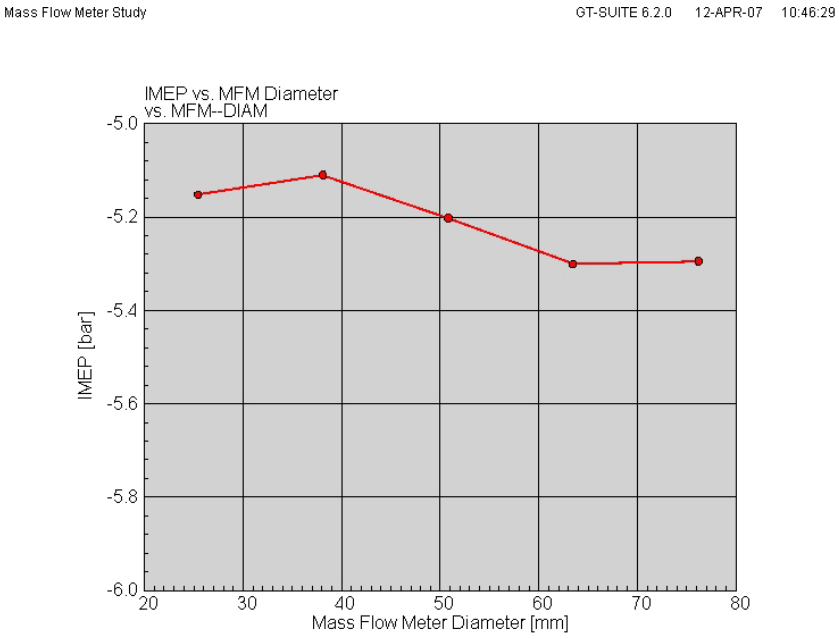

Figure 1.2.2.4. IMEP vs. MFM Diameter

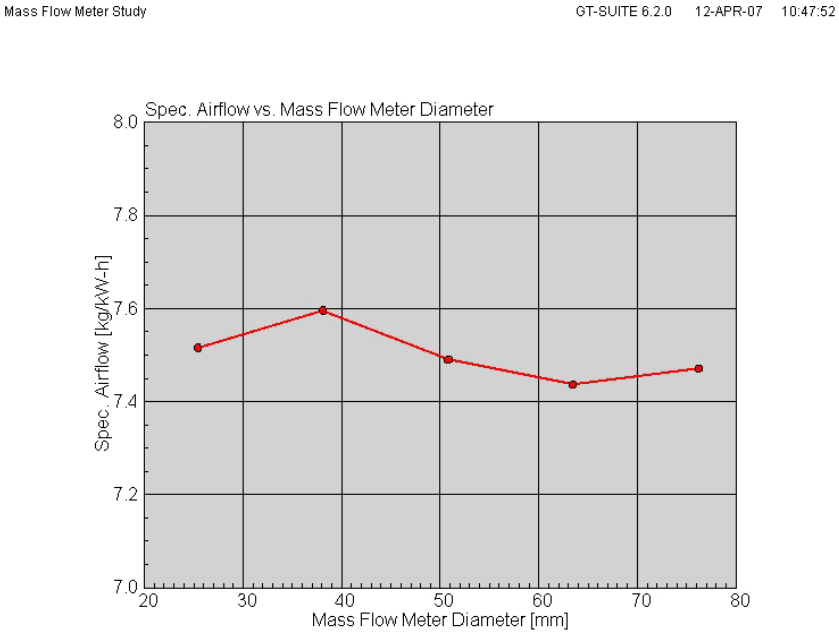

Figure 1.2.2.5. Specific Airflow vs. MFM Diameter

1.2.3 Time Required to Charge Air Tank in AC Mode at 1800, 1500 and 1200 RPM at Selected Values of Exhaust Valve Open (EVO) Timing

The upgraded model, as described in Section 1.2.2 on the mass flow meter was used in this study, assuming that the mass flow meter convergence/expansion was zero, i.e., the pipe section was of constant inner diameter equal to 76.2 mm. For heat transfer, cylinder surface temperatures were selected to be typical of non-combustion conditions, i.e., cylinder wall at 370 K, cylinder head and piston top at 450 K. It was assumed that the exhaust manifold and the piping to the Air Tank were completely insulated.

Figure 1.2.3.1 shows the intake and exhaust valves lifts, the latter relative to allowable lift required to maintain the 1 mm clearance requirements, at 1800 RPM. The exhaust lifts of all EVO timings studied are shown in the figure. The figures would be similar for 1500 and 1200 RPM but would have an earlier EVC to maintain the required clearance. The actual values of EVC employed were –5, -6, and –7.5 deg BTDC for 1800,1500, and 1200 RPM, respectively.

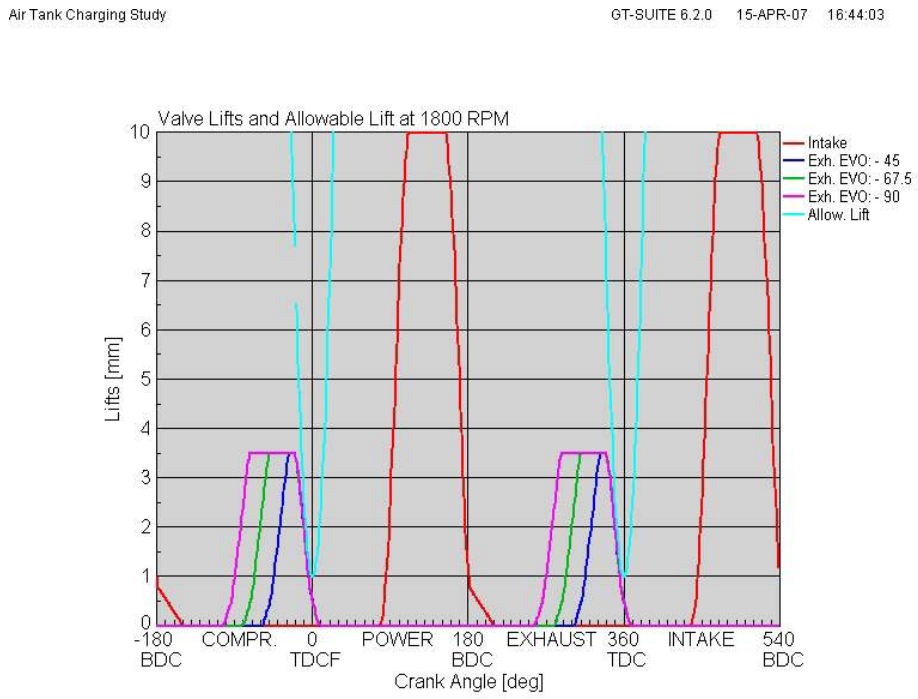

Figure 1.2.3.1. Valve Lifts and Allowable Exhaust Valve Lift at 1800 RPM

The remaining figures show the pressure and temperature vs. time and the instantaneous efficiency vs. time of the AC charging process for 1800, 1500 and 1200 RPM. Keeping EVO constant during the charging process involves a transition from AC1 (blowdown from the cylinder into the Air Tank), through near equilibrium, to AC2 operation (blowdown from the Air Tank to the cylinder). Using equilibrium timings during the entire process would shorten the time required and result in lower final Air Tank temperatures. This could be reasonably well simulated by determining 4 or 5 equilibrium EVO's between 1 bar and 16 bar of pressure and interpolating EVO between these points as the charging process simulation progresses.

At all three RPMs studied, the least time to charge to 16 bar was at an EVO of –90 deg BTDC. At the point when Air Tank pressure exceeds cylinder pressure and flow from the Air Tank to the cylinder begins to occur at EVO, the recompression produces the most rapid (but inefficient) pressure rise. At a timing of –90 deg BTDC this phenomenon occurs earliest in the process.

It should also be noted that these simulations produce a wealth of additional data (e.g., BMEP, torque, specific airflow etc. as a function of time, which are not shown in this report.

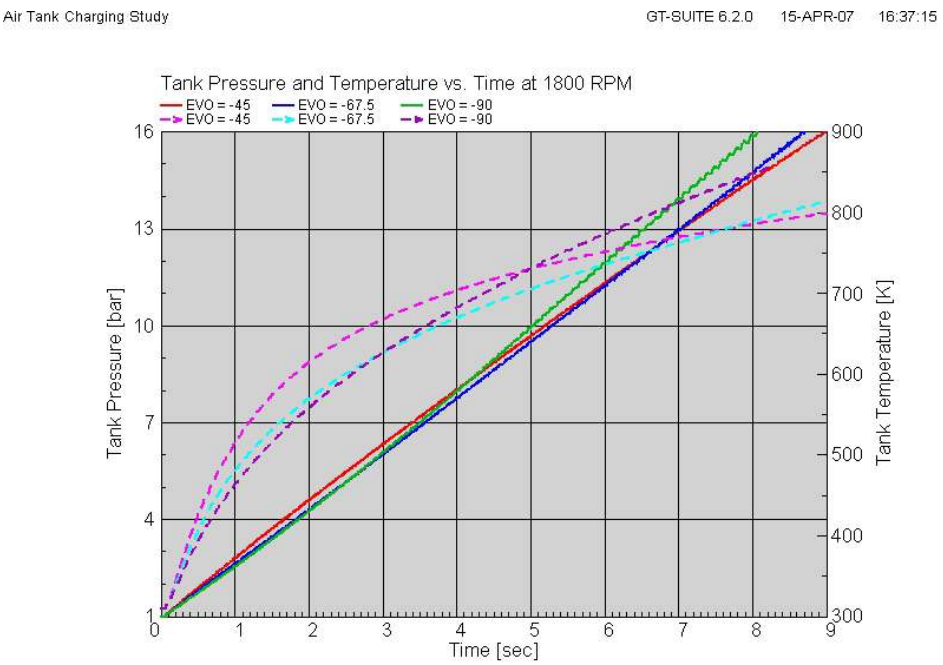

Figure 1.2.3.2. Air Tank Pressure and Temperature at 1800 RPM at Selected Values of EV0

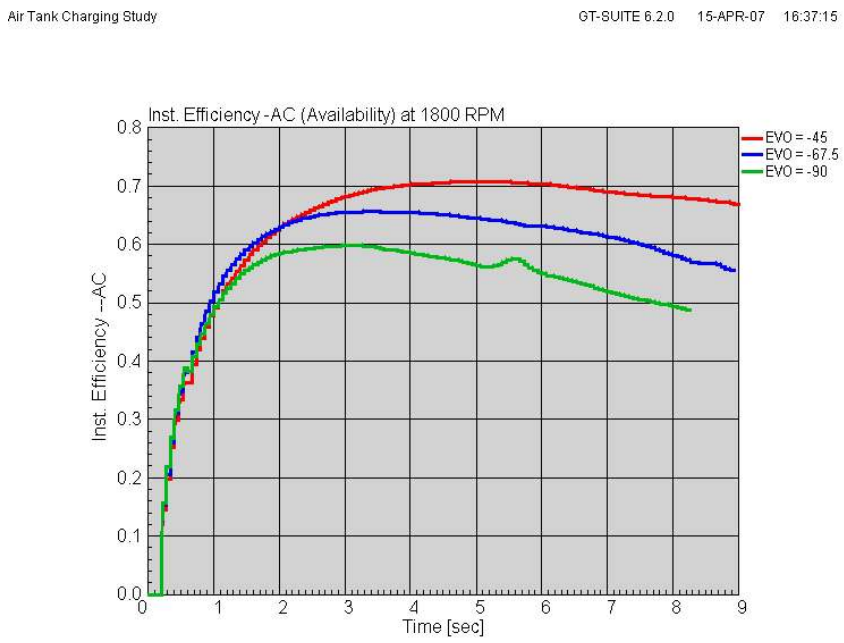

Figure 1.2.3.3. Instantaneous Efficiency During AC Charging at 1800 RPM

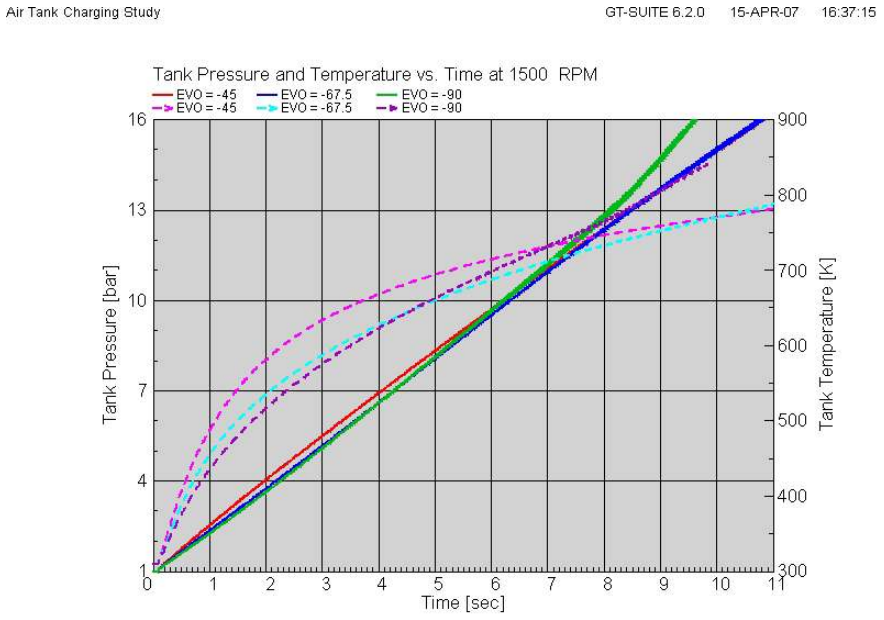

Figure 1.2.3.4. Air Tank Pressure and Temperature at 1500 RPM at Selected Values of EVO

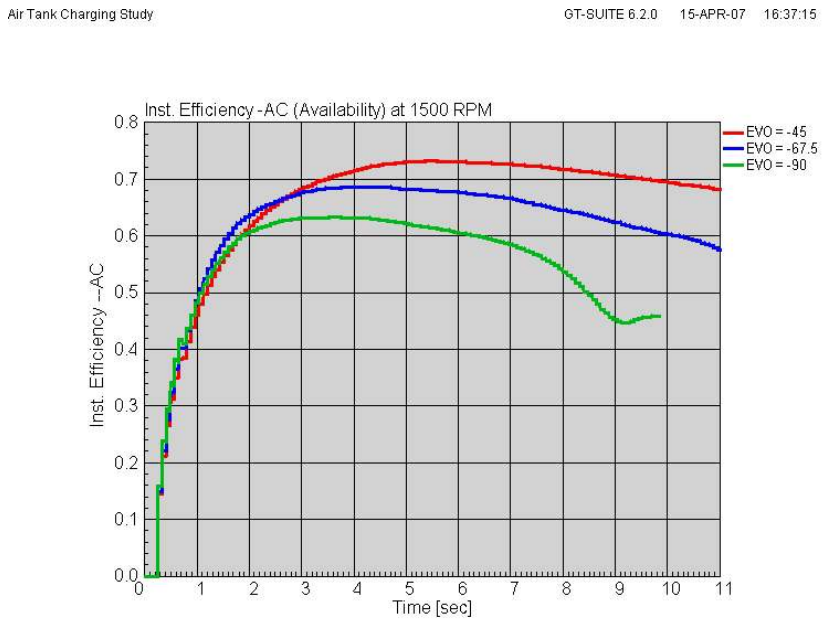

Figure 1.2.3.5. Instantaneous Efficiency During AC Charging at 1500 RPM

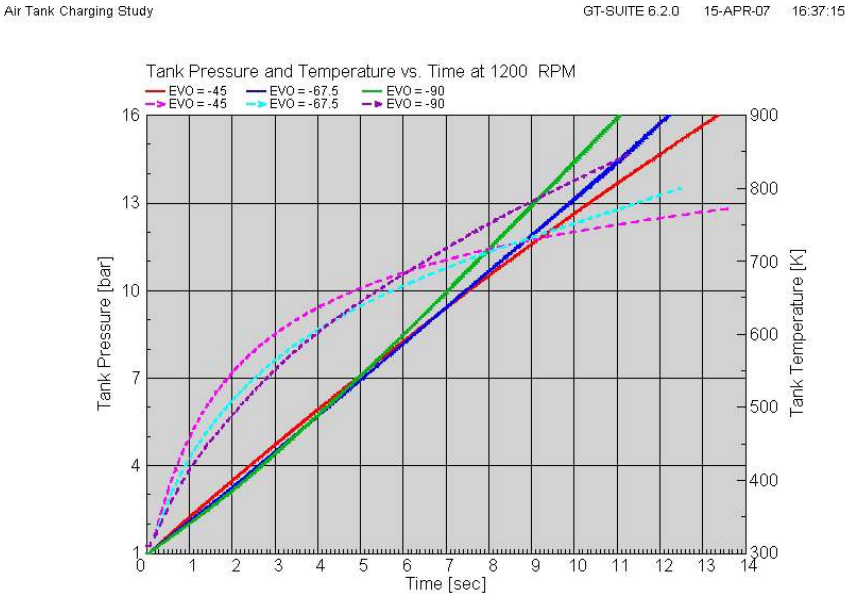

Figure 1.2.3.6. Air Tank Pressure and Temperature at 1200 RPM at Selected Values of EVO

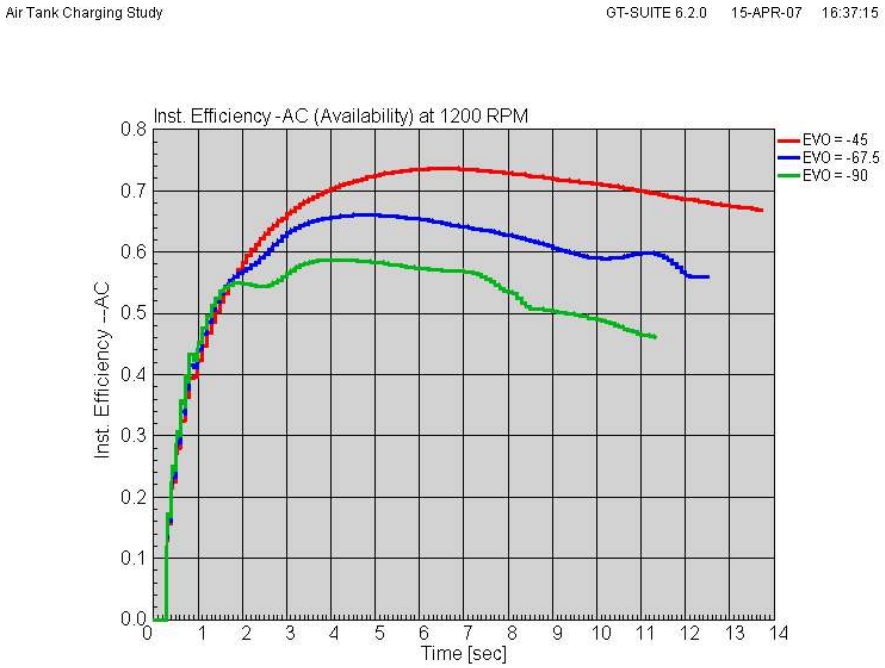

Figure 1.2.3.7. Instantaneous Efficiency During AC Charging at 1200 RPM

1.2.4 Transient AM Operation with 1 and 6 Cylinders Active

An additional modification was made to the GT-Power Pneumatic Hybrid (APA) code so that transient runs could be calculated using all six cylinders or any number of active cylinders less than six. When a cylinder is deactivated the valves are always closed. The addition of this feature was necessary so that the pressure of the finite volume Air Tank (297 liters) would not increase or decrease too rapidly during the AC/AM experimental runs, thereby increasing the difficulty of obtaining accurate data. The valve timings in the code were programmed to be a function of Air Tank pressure during the transient. Unfortunately, due to experimental difficulties associated primarily with the HVA system operation, these experiments were not carried out.

Figure 1.2.4.1 shows the simulated results (pressure, BMEP, efficiency) for a smoothly decreasing mid-level BMEP at 1200 RPM in AM mode for both 6- and 1-cylinder operation in “time-normalized” form to better show the differences and similarities of running with either one or six cylinders. The valve-timing schedule is shown in Figure 1.2.4.2 and is derived from the UCLA “equilibrium” mapping results.

As can be seen from the text label on Figure 1.2.4.1, the absolute time available for discharge is about 5 times greater with only one cylinder running than with six (~24 sec vs. ~5 sec). Also note that with one cylinder, the BMEP becomes negative toward the end of the transient as the Air Tank pressure decreases and that it would be difficult to calculate or verify efficiency from relatively crude dynamometer torque measurements. In-cylinder pressure data vs. CA for P-V integration would be required.

The BMEPs have been adjusted for the friction of the number of active/inactive cylinders and include the power consumption of the HVA system for the active cylinders. BMEPs could also be calculated without the HVA power if this power is not derived from engine output during the testing.

In general, the calculated efficiencies are significantly higher for 1-cylinder operation than for 6-cylinder. Efficiencies are based on indicated work and the relatively high engine friction of the 1-cylinder case has no effect on this number. Therefore, the higher efficiencies are most likely due to the smaller flow restriction at the lower flow rates typical of 1-cylinder operation. They may also be due to the fact that the optimal valve timings are different for 6-cylinder operation than for 1-cylinder operation. This latter effect was not investigated thoroughly.

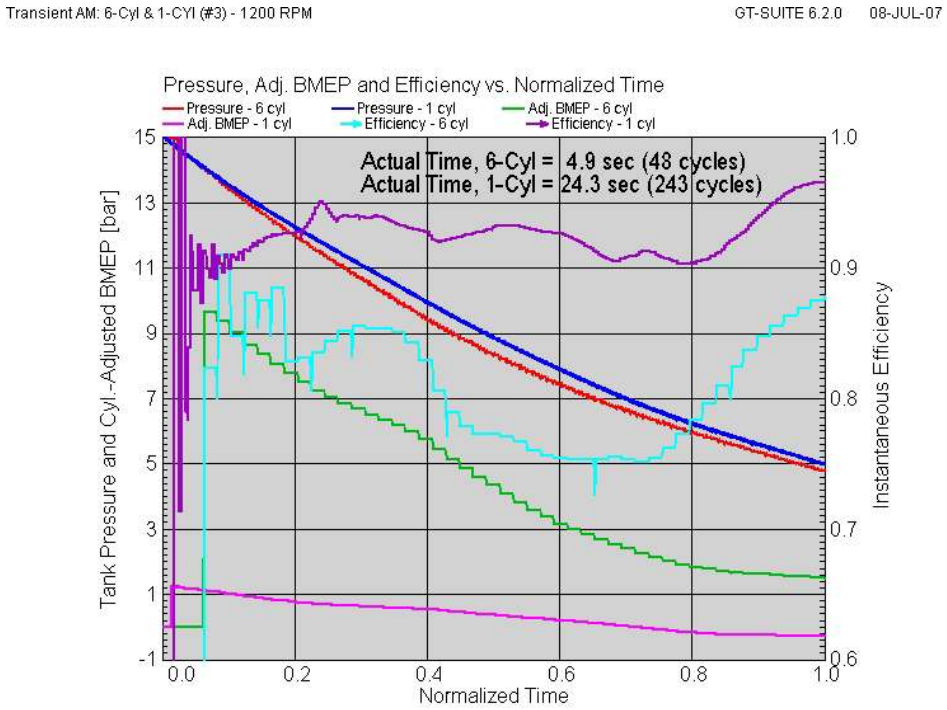

Figure 1.2.4.1. Air Tank Pressure, BMEP and Efficiency vs. Normalized Time

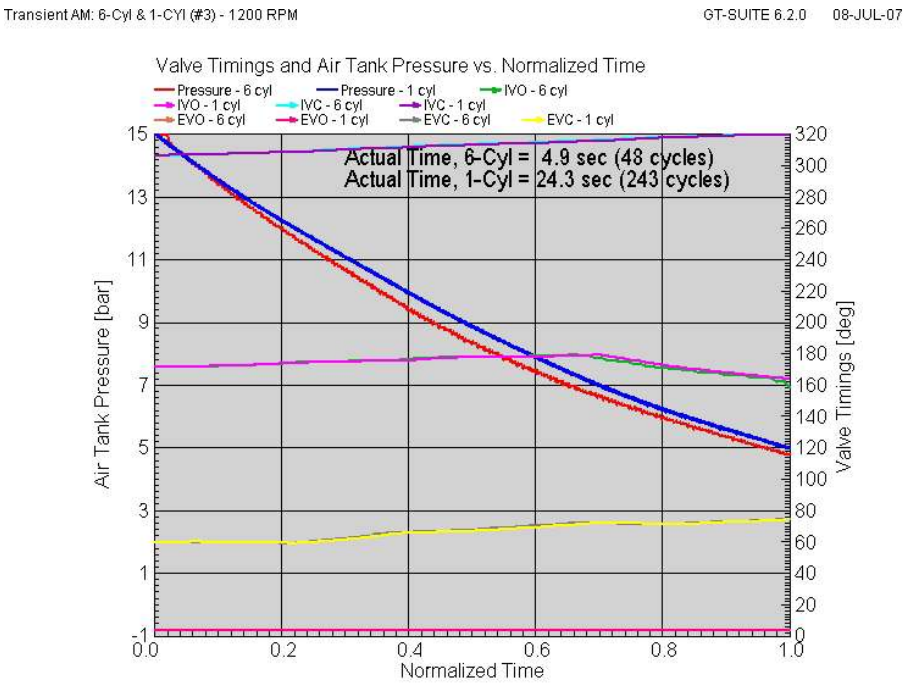

Figure 1.2.4.2. Air Tank Pressure and Valve timings vs. Normalized Time

1.2.5 Air Tank Temperature During Equilibrium Air Charging (AC Mode) at 1200 RPM with Pressure Regulation at 15 bar

Figure 1.2.5.1 shows the Air Tank temperature and pressure, along with other system temperatures of interest for a 6-cylinder AC charging event at 1200 RPM and approximately 8.5 bar Air Tank pressure. Pressure regulation is imposed to prevent buildup of excessive pressure in the tank. The initial pressure of the simulation is slightly below 15 bar, i.e., 14.9 bar. The initial temperature is at the adiabatic temperature corresponding to 15 bar, i.e., ~627 K. The purpose of the simulation is to determine steady-state temperature under pressure regulation.

The valve timings applicable to Figures 1.2.5.1 and 1.2.5.2 are near-equilibrium values as shown below:

EVO	EVC	IVC	IVO	
302.3	**356.0**	**188.5**	**71.2**	**(Crank Angle Degrees)**

The results show that the regulator maintains 15 bar pressure and that the temperature approaches the inlet temperature to the Air Tank. Since the tank is regulated at 15 bar pressure, there is always an intermittent outflow through the regulator valve which ultimately must equal the inflow at steady-state. The final steady-state Air Tank temperature approaches the inlet temperature from the pipe to the Air Tank. From a fundamental perspective, the Air Tank acts like a well-mixed volume or pipe element in the flow between the inlet pipe and the outlet from the regulator and its pressure and

temperature approach that of the flow into it. The average pressure of the flow into the Air Tank (which is not shown) is essentially 15 bar.

In Figure 1.2.5.1, in addition to Air Tank T & P, the adiabatic temperature at 15 bar (627 K), the final value of the outlet temperature from the pipe which connects to the tank (which is very close to the steady-state maximum Air Tank temperature) and the final value of the exhaust manifold outlet temperature are also shown. The exhaust manifold outlet temperature is a little lower than the temperature of entry to the tank even though the pipe is 100% insulated most likely due to the pressure drop over the long length of the pipe. This pressure loss is converted to heat raising the temperature by a few degrees.

One apparent conclusion is that the maximum temperature reached in the Air Tank will be governed by engine conditions, in particular, choice of valve timing. As will be seen in section 1.2.6, the situation is different for a long run starting at lower pressure where the pressure in the tank builds up over time. It will also be different if the valve timings are conducive to the rapid development of high temperature, also shown in Sections 1.2.6 and 1.2.7.

Figure 1.2.5.2 also shows that since there is no change in Air Tank pressure or temperature after reaching a steady state and, consequently, no increase in thermodynamic availability of the tank contents, the efficiency is zero. Therefore, steady-state Air Tank conditions cannot be used as a measure of efficiency in this type of experiment.

INTENTIONALLY LEFT BLANK

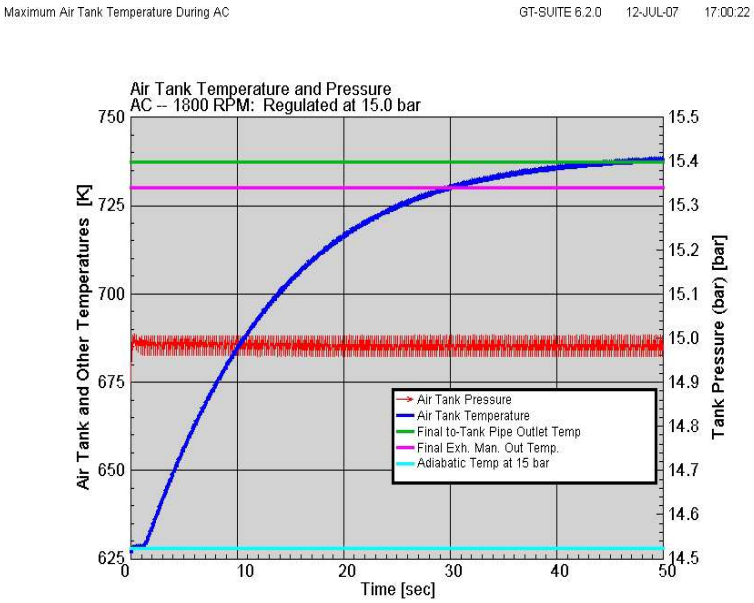

Figure 1.2.5.1. Air Tank Temperature and Pressure vs. Time (Other System Temperatures Also Shown)

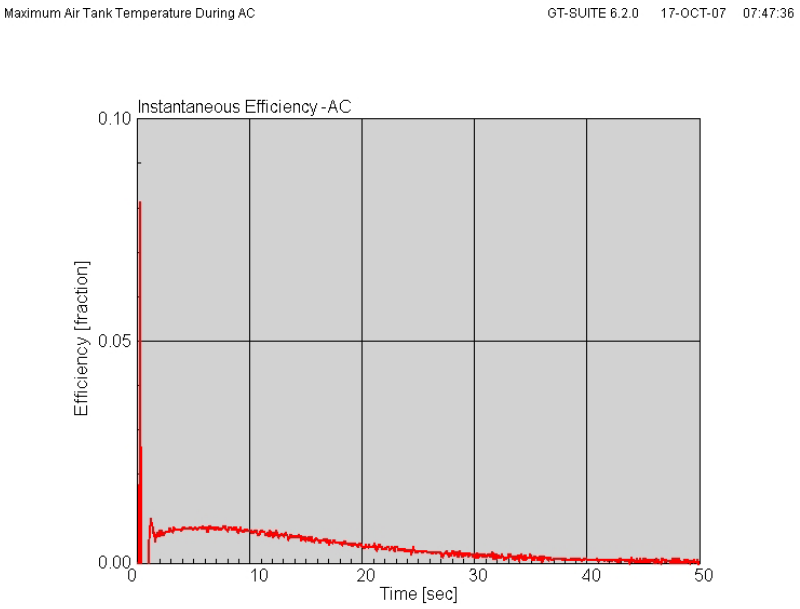

Figure 1.2.5.2. Efficiency vs. Time for the Pressure-Regulated AC operation of Figure 1.2.5.1

1.2.6 Air Tank Temperature During High Recompression Operation (AC2) at 1200 RPM with Pressure Regulation at 15 bar

Figure 1.2.6.1 shows the effect of exhaust valve timing on Air Tank temperature. All conditions are the same as the previous study except that EVO is set early to 240 deg BTDC. This exhaust valve timing introduces a high degree of recompression as air flows out of the tank and is compressed again in the engine cylinders. Starting at 14.9 bar and the corresponding adiabatic temperature in the Air Tank (627 K), the temperature in the Air Tank rises to nearly 800 K in ~6 seconds, on its way to 1040 K, which would be the final temperature even though the pressure is regulated to 15 bar. This could be a hazardous condition in terms of the material strength of the Air Tank.

Thus, valve timing choice as well as pressure regulation must be considered in performing experiments.

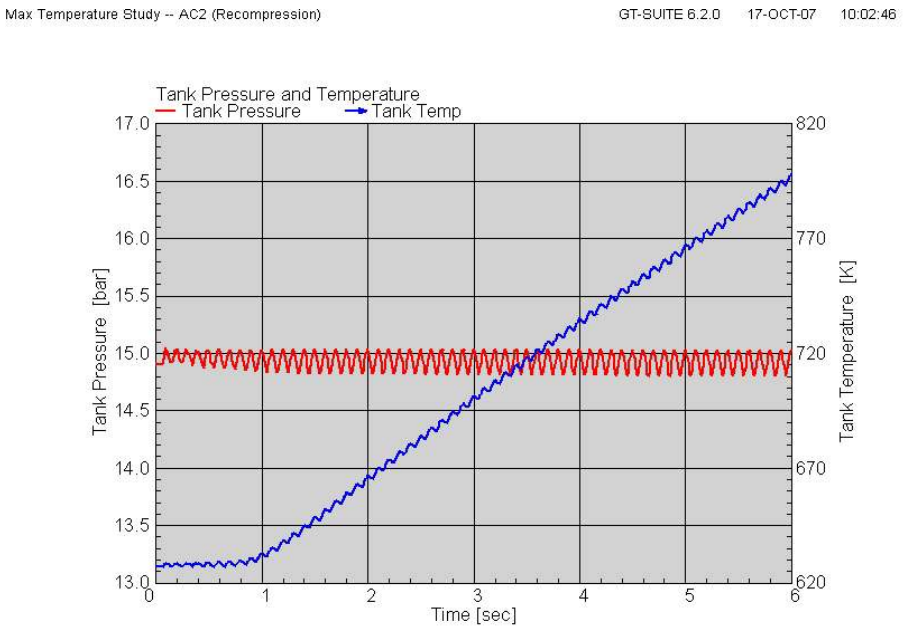

Figure 1.2.6.1. Air Tank Temperature and Pressure vs. Time for a High Recompression AC Operating Mode at 1200 RPM

1.2.7 Near-Equilibrium and Irreversible Charging at 1800 RPM

Figure 1.2.7.1 shows the comparison between charging the Air Tank from atmospheric pressure to a regulated pressure of 10 bar at 1800 RPM under both “near equilibrium” conditions and highly irreversible conditions, the latter characterized by significant recompression of previously stored air in the cylinders (AC2 operation).

It can be seen that even with pressure regulation highly irreversible charging can lead to potentially hazardous temperatures of over 800 deg K in a short period of time. This

emphasizes the need for well-defined valve timing strategy during charging as well as the ability to control the operation of the HVA system in accord with the strategy.

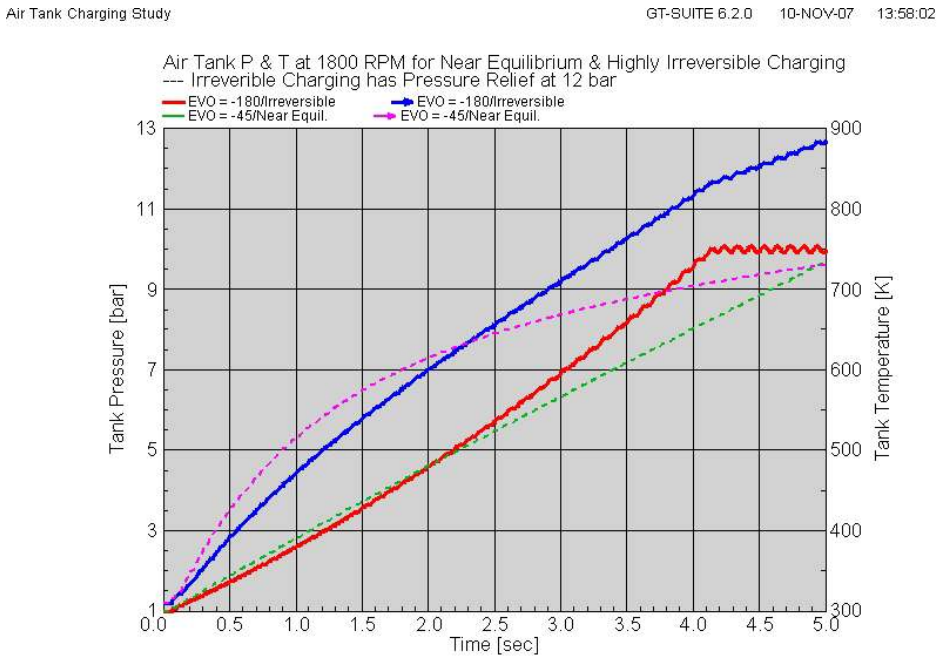

Figure 1.2.7.1. Pressure and Temperature vs. Time Compared for “Near Equilibrium” and Highly Irreversible Air Tank Charging from Atmospheric Conditions at 1800 RPM with 10 bar Pressure Regulation.

1.2.8 Simulation vs. Experiment for AC at 800 RPM Steady State

After the experimental and control equipment was assembled in the test cell, a variety of tests were run. They are described much more fully in other sections of the Phase III report.

One set of steady-state AC runs at 800 RPM at 3 and 5 bar Air Tank pressures was simulated using the multicylinder model to determine the degree of agreement with experimental results for both torque and measured airflow. In these experiments, EVO was varied, as it is a critical parameter controlling the level of negative torque absorbed by the engine.

Figures 1.2.8.1 and 1.2.8.2 show the comparisons in torque and airflow respectively.

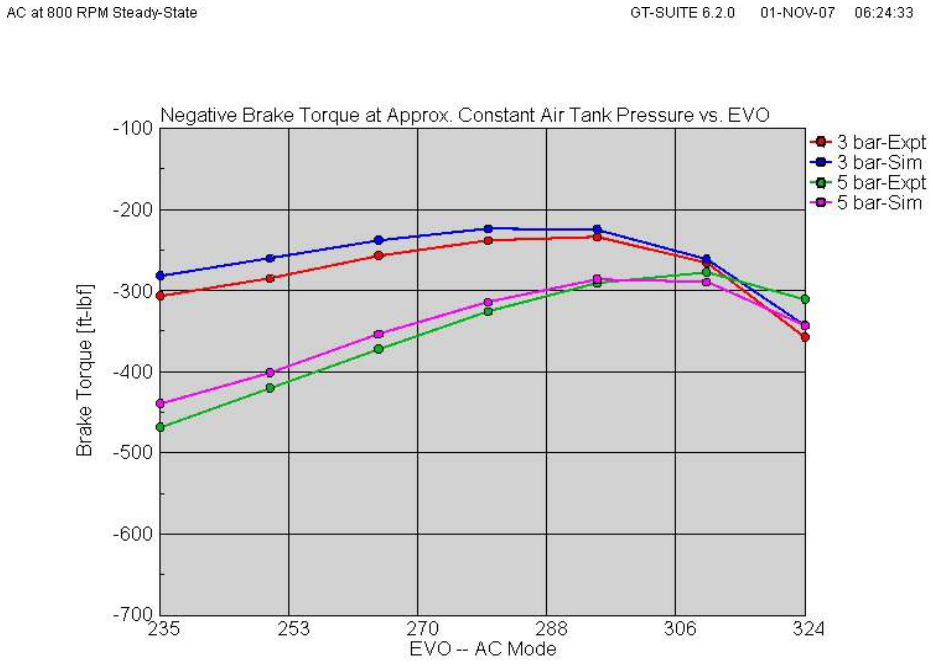

Figure 1.2.8.1. Measure and Predicted Brake Torque as a Function of EVO at 800 RPM and at Air Tank Pressures of 3 and 5 bar.

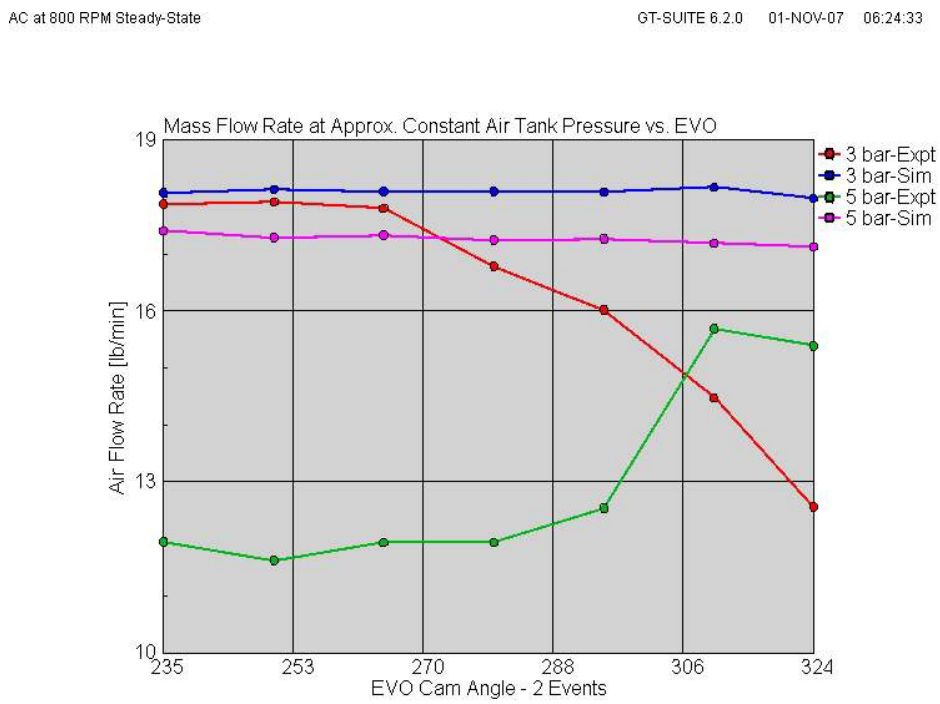

Figure 1.2.8.2. Measure and Predicted Air Flow as a Function of EVO at 800 RPM and at Air Tank Pressures of 3 and 5 bar.

It can be easily seen that the agreement in torque between experiment and simulation is quite good. This is due to the fact that the torque is almost exclusively determined by the in-cylinder pressures. Airflow, on the other hand can be greatly affected by air leakage past valves and any other sources of leakage. In principle, the airflow should be a function that is largely dependent on engine speed, engine displacement and the pressure level in the tank since, in AC mode, these quantities determine the air displaced from the cylinder to the Air Tank and the variation with EVO should be small. As is evident from Figure 1.2.8.2 the simulated airflow shows this trend whereas the measured airflow is generally lower than predicted and exhibits an erratic trend not easily explained.

Airflow can be greatly affected (i.e., reduced in AC mode) by leakage across the exhaust valves of the system, as will be discussed more thoroughly later. The lack of agreement in airflow, along with inability to charge the Air Tank to high pressures and the physical inspection of the HVA components after testing were significant contributors to diagnosing the experimental issues as being related to air leakage across the exhaust valves.

1.2.9 Simulated AC Charging at 800 RPM/ EVO 280 deg BTDC Comparing Fully Seated, Leaking Exhaust Valves and Simulated Valve Guide Leakage – Initial Conditions: Ambient

Shortly after the start of experimental dynamometer work it became apparent that there was a difficulty in charging the Air Tank in AC mode to the expected pressures of 10 –12 bar. Various leaks in the exhaust system to the Air Tank and through the compressor bypass valve were detected and fixed but the problem persisted. It soon became evident that it was necessary to check the detailed operation of the HVA system, particularly the exhaust valve. The exhaust valve has to withstand very high back pressures and it was essential to determine whether it was operating as intended and fully sealing the cylinder when it was supposed to be closed.

In an effort to diagnose the experimental difficulties encountered in AC charging, i.e., inability to reach elevated Air Tank pressures, the GT-Power model was modified to 1) accept experimental valve traces; and 2) to allow for the exhaust valves to be either fully seated during normally closed periods or to have a small leakage lift during these periods. In addition two orifices, with specifiable diameter, were inserted in the exhaust manifold discharging to ambient to simulate valve guide seal leakage. Due to the limitations of GT-Power, this is an imperfect simulation since it disconnects the source of the air leakage (i.e., the cylinder) from the flow but it does establish a path to the ambient, which was considered a reasonable approach.

Figure 1.2.9.1 shows the valve lift profiles used in all 3 cases – case 1) no leakage of any kind; case 2) leakage due to the exhaust valves not being fully seated (0.2 mm leakage lift); and case 3) leakage due to valve guide seals simulated by two orifices to ambient on opposite sides of the exhaust manifold, each of 7.5 mm diameter. These diameters for the valve guide leakage were highly amplified compared to the flow diameters of paths that would be encountered if valve guide leakage were a problem. The intake lift profile was the same for all three cases.

Figure 1.2.9.2 shows the Air Tank pressure charging vs. time for the 3 cases studied. The "no leakage" case shows linear charging that could easily charge very rapidly to pressures well above 12 – 14 bar. Both the "leaky" exhaust valves and the simulated valve guide seal leakage curves show that high pressures cannot be attained and that the Air Tank pressure approaches an asymptotic value, in this case about 7.5 bar for the leakage parameters chosen.

However, it is very implausible that valve guide leakage would be as much as that predicted by two orifices of 7.5 mm each, which is a very large leakage area compared to that of valve guides that are not 100% sealed. On the other hand, a constant 0.2 mm leakage lift for the exhaust valves is a plausible simulation of exhaust valves that are not closing fully, open dynamically at specific times when they should be seated and other abnormalities in operation.

Therefore, it was tentatively concluded that the inability to reach high pressure during experimental AC charging runs was due to the exhaust valve leakage rather than valve guide seal leakage. This also corresponded to data obtained on the APA engine at Volvo Powertrain in which a relatively small valve guide leakage was measured.

Figure 1.2.9.3 shows the specific airflow for the 3 cases. Although they all decrease as Air Tank pressure increases, the trends are quite different due to the different phenomena that take place in each of the cases. For the "no leakage" case, the airflow decreases due to the natural buildup of Air Tank pressure and the back flow into the cylinder as the Air Tank pressure begins to exceed the compression pressure at the EVO setting. When the exhaust valves are "leaky" the backflow due to compression in the cylinder begins to approach the inflow quite early and eventually goes to near zero as the two equalize and the asymptotic pressure is reached. Compressed air essentially leaks from the Air Tank through the exhaust valve into the intake system, during the period when the intake valve is open, thereby inhibiting the induction of additional air for compression. For the case of simulated valve guide leakage, the mechanism is leakage to ambient, which offsets backflow from the cylinder. This allows a higher value of airflow (compared to the "leaky" exhaust valves) even at the asymptotic value of the Air Tank pressure. At a true steady state, the airflow into the engine will equal the simulated valve guide seal leakage.

However, valve guide leakage was eliminated as a possible mechanism for the inability to charge during AC due to the very large orifice diameters used in the simulation (compared to physically possible leakage path dimensions) and the experimental observations that the valve guide air leakage was small. Therefore, major attention during subsequent teardown and evaluation was focused on exhaust valve operation.

INTENTIONALLY LEFT BLANK

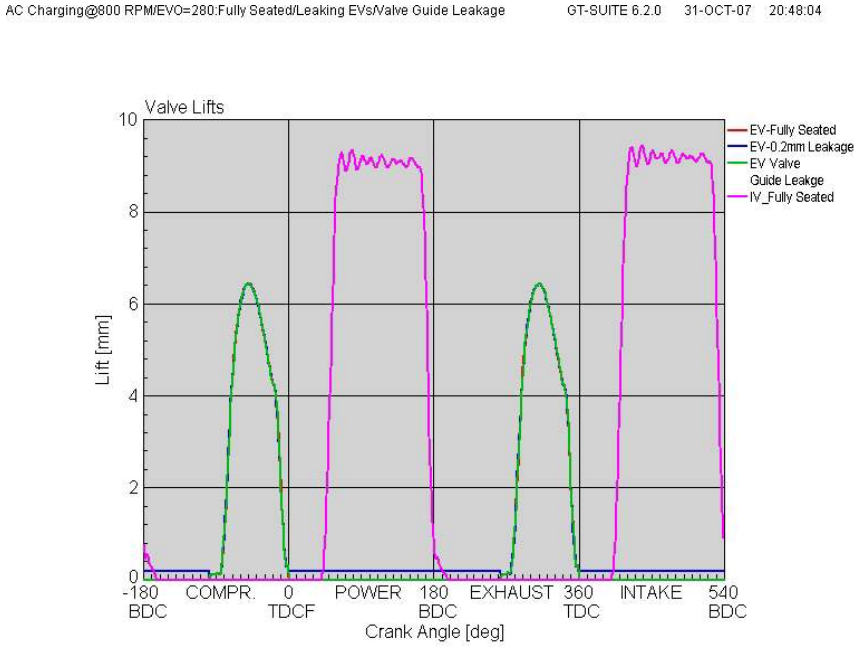

Figure 1.2.9.1. Valve Lift Traces for the 3 Cases Simulated

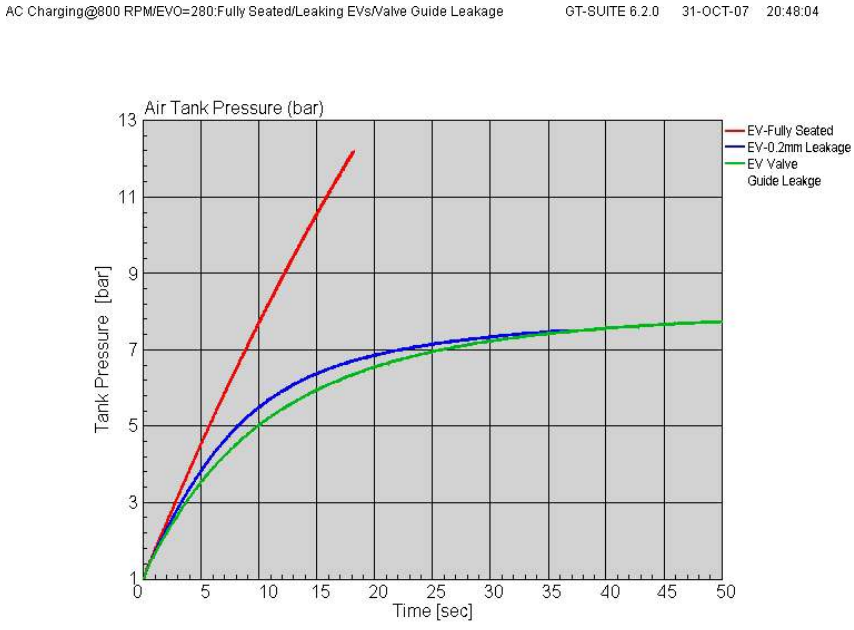

Figure 1.2.9.2. Air Tank Pressure vs. Time for the 3 Cases Simulated

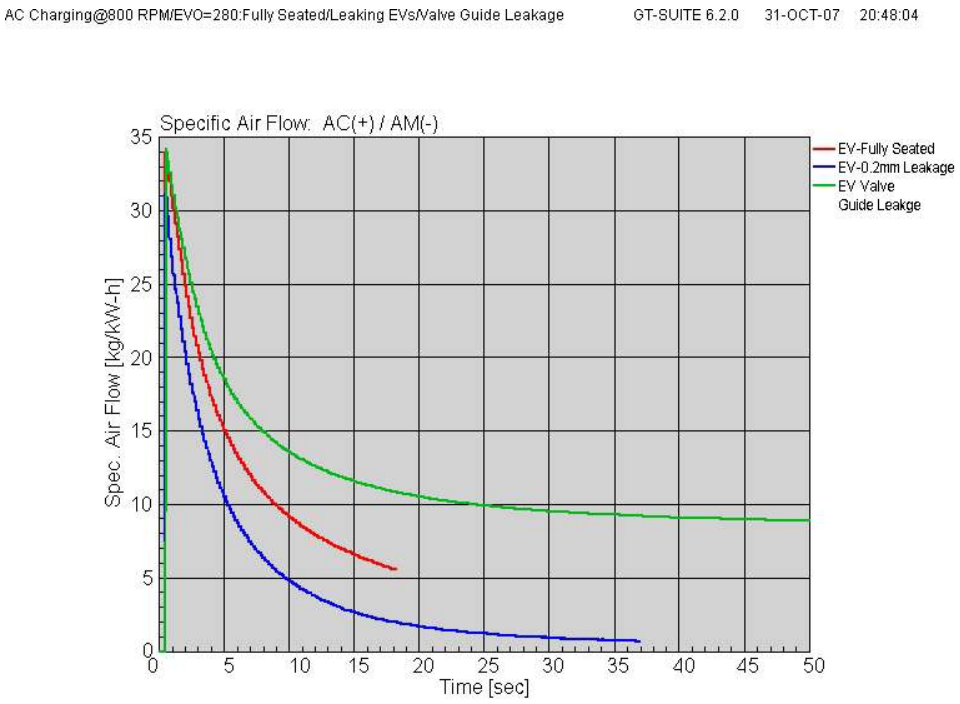

Figure 1.2.9.3. Specific Air Flow as a Function of Time for the 3 Cases Simulated

1.2.10 AC Charging with Constant 0.15 mm Exhaust Valve Lift Leakage Combined with 25% Intermittent Extended Exhaust Valve Landing Tail (same conditions as in Section 1.2.9)

Another phenomenon observed from the experimental traces of exhaust valve motion was intermittent delayed closing, which occurred under transient valve timing conditions. This is referred to as a landing tail (LT). LTs were observed with lifts of up to 1 mm and typical durations of 80 degrees crank angle. In addition to the constant exhaust leakage due to lack of full seating, the LT creates a direct path (during valve overlap) from the high-pressure air storage system to the low-pressure intake system, inhibiting the intake and compression of air.

To simulate this, a combination of extended LT events at 25% frequency (representative of the data) was combined with a small constant EV leakage represented by 0.15 mm of leakage lift during the time when the valves were to be fully seated. This is an obvious simplification, but the objective was to capture the essence of the phenomenon.

Figure 1.2.10.1 shows the valve lift profiles assumed for this case, showing both the extended tail and the constant leakage lift during the rest of the cycle when the EV should be closed. This lift profile is employed for 25% of the cycles. Although not shown, for the remaining 75%, the EV lift profile shows no extended LT but exhibits a constant leakage lift of 0.15 mm.

The Air Tank pressure vs. time simulation using the 25% frequency factor for extended LTs combined with a constant EV exhaust valve leakage is shown in Figure 1.2.10.2. It reaches a fairly low asymptotic value, typical of experimentally obtained results.

Thus, it appears quite plausible that both of these problems in the HVA system played a significant role in preventing charging to high pressure and the subsequent inability to collect accurate data over a wide range of operating conditions.

INTENTIONALLY LEFT BLANK

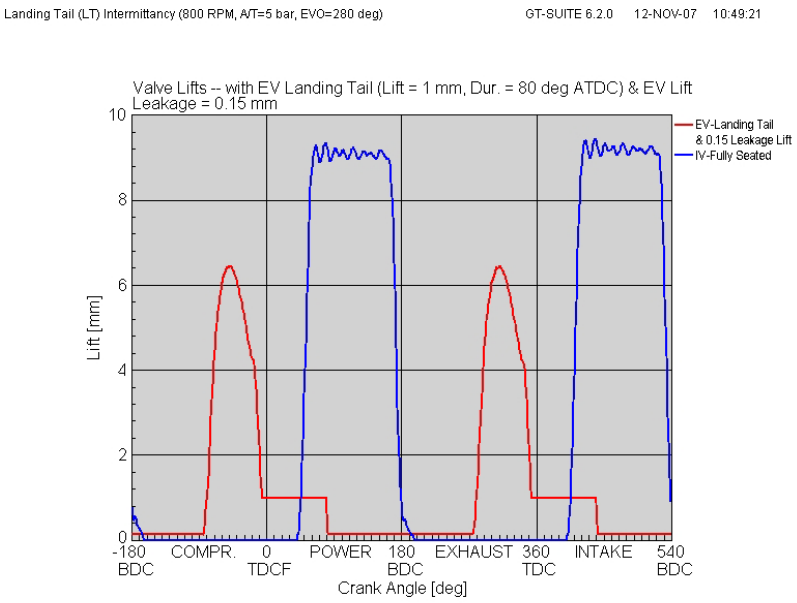

Figure 1.2.10.1. Exhaust Valve Lifts with 80 Degree EV Landing Tail and 0.15 mm Constant Seating Leakage.

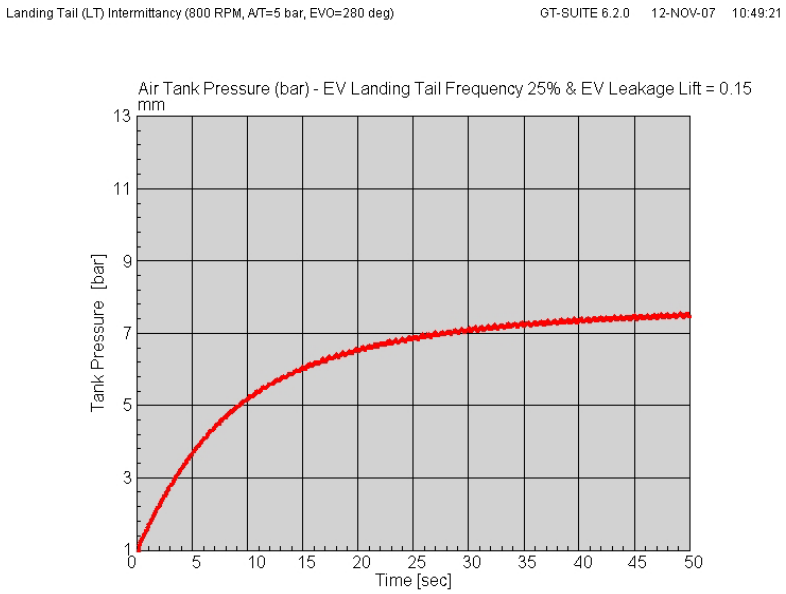

Figure 1.2.10.2. Air Tank Pressure vs. Time for 25% Frequency of Extended EV Landing Tails Combined with a Constant 0.15 mm of Exhaust Valve Lift Leakage.

1.3 Summary and Conclusions

Detailed multicylinder and single cylinder pneumatic (air hybrid) system models were developed, modified and refined during the DOE/Mack/Volvo Powertrain APA program. They were used extensively, as illustrated in the final report and the reports for the earlier phases. They proved to be indispensable tools for both predictive and diagnostic purposes and, in general, to derive a better understanding of the operation of the complex and dynamic APA system as a whole. In Phase III, the models were instrumental in identifying some of the key issues with the experimental HVA system, which contributed to the difficulties in acquiring fully accurate data.

Considering the complex, multivariable nature of the APA system, it is difficult to envision carrying out a well-structured program without such models. Some of the specific applications of the APA system models that can be highlighted are:

1. Understanding complex phenomena such as gas dynamics and cylinder pulsation effects on performance.

2. Assisting in design of components such as: APA EV maximum lift specification; less restrictive exhaust manifold; expected temperatures in the Air Tank under various charging scenarios; intake temperature thermal requirements during AM; and the air storage system air flow meter.

3. Allowing for systematic mapping of engine in APA modes (AC and AM) and determination of efficiency optima and corresponding valve timings prior to operational hardware availability.

4. Assessing safety issues related to pressure and thermal stress prior to operation.

Understanding at an early and fundamental level the potential effects on the experimental results of various hypothesized HVA malfunction.

INTENTIONALLY LEFT BLANK

2 Control Subsystem Development and Test Cell Experiment

Summary

In the control subsystem development, the sensor and actuator signals required for APA engine control and for measuring power conversion efficiencies are first analyzed. Sensors are then calibrated and installed. The controller employs a 2-level structure. The high level controller is based on the on the ETAS ES1000 prototype platform and its function is to schedule engine running modes and determine valve timings under each mode. The algorithm is developed in the ETAS ASCET environment. At the core of the algorithm are the timing maps developed during Phase II. The lower level controller consists of the HVA controller and air switching valve drives. The upper and lower level controllers communicate through CAN bus. In the system integration, hardware-in-loop simulations are conducted to verify the operations of the engine valves and air switching valves. The data acquisition system is designed to guarantee data synchronization and provide convenient data structure for test analysis.

The prototype APA engine system is integrated for test-cell experiment. AC steady state tests and AC-AM transient tests are conducted for various pressure, speed and load conditions. The test results are analyzed for engine torque generation and cycle efficiency. Diagnostic tests and analysis are performed to identify the causes of some problems encountered in the experiment

2.1 Conclusions of Phase III

From the work of the control sub-system development, the APA experimental system integration, test, and test result analysis, the following conclusions can be drawn:

(1) The control sub-system satisfies the requirements of the APA engine testing;

(2) The APA engine experimental system has been established;

(3) The operation of APA has been successfully demonstrated experimentally;

(4) The torque generation through the engine valve control agrees very well with the Phase II simulation results;

(5) The efficiency of APA operation and the achieved pressure are much lower than the simulation results, and the reason is primary due to the exhaust valve actuation; other factors, such as leakage and heat loss, also contribute;

(6) Fully flexible valve actuation and handling of high pressure and temperature air are the main technical challenges to promote APA technology.

2.2 Summary of Project: Air Power Assist Engine Modelling, Simulation, Control System Development, System Integration and Testing

In Phase I, the structure configuration and selection for applying the air power assist (APA) concept to the MD11 engine was first completed. The MD11 APA engine model was developed using GT-Power and preliminary mapping results were obtained for simplified evaluation of braking energy recovery. Initial work on the optimization of the valve timings was also performed.

In Phase II, the work of APA engine modeling, simulation, and mapping was continued as updated and more accurate information became available. In the modeling, valve discharge coefficients were identified to be critical to the efficiency computation for the hybrid operation; as such new sets of coefficient data were obtained and included in the model to study the effect of exhaust valve lifts on efficiencies; updated valve profile, valve actuation system power consumption, and air handling components' thermal limits were obtained from the hardware development team to improve the model. In the simulation and mapping, a new search algorithm was developed for accurate valve timing optimization. A user defined program was developed to integrate this algorithm into GT-Power and to automate the search data logging. Finally, based on these studies and development, the detailed engine mapping of the Air Compression (AC) and the Air Motor (AM) operations was completed.

The Phase III effort was directed to integrating the experimental system and testing. In the control subsystem development, the sensor and actuator signals required for APA engine control and for measuring power conversion efficiencies were first analyzed. Sensors were then calibrated and installed. The controller employed is a 2-level structure. The high level controller is based on the on the ETAS ES1000 prototype platform and its function is to schedule engine running modes and determine valve timings under each mode. The valve timing control algorithm was developed in the ETAS ASCET environment. At the core of the algorithm is the timing maps developed during Phase II. The lower level controller consists of the HVA controller and air switching valve drives. The upper and lower level controllers communicate over the CAN bus. In the system integration, hardware-in-loop simulations were conducted to verify the operations of the engine valves and air switching valves. The data acquisition system was designed to guarantee data synchronization and provide convenient data structure for test analysis. The prototype APA engine system was integrated for test-cell experiment. AC steady state tests and AC-AM transient tests were conducted for various pressure, speed and load conditions. The test results were analyzed for engine torque generation and cycle efficiency. Diagnostic tests and analysis were performed to identify the causes of some problems encountered in the experiment

2.3 Conclusions of Project: Air Power Assist Engine Modelling, Simulation, Control System Development, System Integration and Testing

UCLA participates in the project from the concept discussing in the very beginning of this project to the final testing. UCLA's effort has been devoted to the APA engine concept development, modeling, simulation and experiment verification. The tasks accomplished are summarized as follows:

(7) The structural design of the MD11 APA engine has been completed;

(8) The GT-Power model of the APA engine with realistic considerations regarding engine valve actuation and air handling has been established;

(9) The APA engine operation has been simulated and optimized; and the operation maps have been created based on the simulation results;

(10) The control sub-system has been developed and it satisfies the requirements of the APA engine testing;

(11) The integration of the APA engine experimental system has been completed;

(12) The operation of APA has been successfully demonstrated experimentally;

(13) The torque generation mechanism has been confirmed experimentally and the testing results agree with the Phase II simulation results;

The main results of this project are concluded as follows:

(1) The efficiency of APA operation and the achieved pressure in the experiment are much lower than those predicted by the computer model and simulation. The reason is primary due to uncontrollable exhaust valve motion.

(2) Fully flexible valve actuation and handling of high pressure and temperature air are the main technical challenges for realizing the APA technology.

3 Sturman Industries Post-Installation Report For Volvo/Mack APA System

Summary

The design and fabrication of the Sturman Industries APA HVA system have been described in detail in previous reports.

The Sturman Industries APA HVA system was installed on a MD11 engine at Volvo/Mack in Hagerstown Md. The system was used to conduct engine dynamometer testing in order to validate the performance of the APA system.

During installation the APA HVA system was shown to be operating properly. During the process of the dynamometer testing several issues hardware issues were observed which compromised the performance of the APA HVA system. These issues are described in further detail in this report.

3.1 Conclusions

The HVA system as originally installed on the engine performed as expected. During the course of testing, the valve keeper retainer caps became loose and significantly compromised the performance of the system, by causing the exhaust valves to not seat completely.

For future HVA assemblies, the valve keeper retainer caps becoming loose problem can be avoided with the use of a thread lock compound during assembly.

Due to the end of the APA project the HVA hardware will be returned back to its pre-APA configuration, which uses return springs instead of the APA hydraulic return which should present no further operational issues.

4 Air Handling System

Summary

Air Handling Group designed and delivered hard wares for the APA engine completely on June 2007. Functional testing also completed. In this report, Introduction of air handling components and functional test results will be discussed and summarized.

4.1 Conclusion

Functional Test Results of Air Handling Components for APA engine

- No failures in three-way and compressor bypass valves
  - ✓ Successfully withstood pressures up to 13 bar (three-way valve)
  - ✓ Successfully withstood firing exhaust temperatures (three-way valve)
- Leak rate higher than desired
  - ✓ Air tank leaked down in approx. 2 minutes with valve closed
  - ✓ This was a known risk with a butterfly valve in this size
  - ✓ Recommend re-design with specific exhaust three-way valve (currently common with intake three way valve) which uses smaller butterfly for air-tank side (approx 1” ID suggested)
- Valve response time slower than expected
- The APA 3-way valves and compressor bypass valve must actuate (fully closed to fully open) in 100 ms or less
- The valves tested took between 0.7 – 1.0 sec to actuate
- Root cause has been determined
  - ✓ A minimum air flow of 11 CFM is required to actuate the valves in the time required
  - ✓ Air lines and fittings are too small to supply the required flow rate at high pressure
- Recommendations to resolve issue
  - ✓ Re-design pneumatic actuator with fittings for ¾” air lines
  - ✓ Replace air lines with ¾” hose
  - ✓ Higher capacity air solenoids may also be required
- Manifold performed as designed for the duration of the test.
  - ✓ Successfully sealed pressures up to 13 bar

- ✓ Successfully withstood firing exhaust temperatures

- Air Tank system performed as designed for the duration of the test.
  - ✓ Successfully stored pressures up to 13 bar
  - ✓ Air tank pressure regulator functioned as expected
  - ✓ Air tank flow meter functioned as expected
  - ✓ Air tank hose failed
    - Rubbed-through against sharp edge: installation fault
    - Repairs were affected and testing resumed

INTENTIONALLY LEFT BLANK

5 Air Hybrid Engine Inlet and Exhaust Valve Evaluation

5.1 Summary - Inlet and Exhaust Valve Evaluation

1. Piston to valve contact caused a failure of the valve guide and will cause a valve bending fatigue failure with longer test time.
2. Valve seat leak will cause damage to valve and valve failure with longer test time.
3. Valve stems were scuffed and would cause excessive guide wear in longer tests.
4. The upper valve guide cracked. This failure was possibly due to misalignment.

INTENTIONALLY LEFT BLANK

6 Estimation of vehicle fuel economy

The ADVISOR simulation model needs the steady state air flow rates to calculate the energy in the storage tank. While in Phase I and II, the air flow rates were readily available and were used to predict the driving cycle fuel economy improvement, the air flow rates from the experiment are sparse and the AM steady state flow rate is lacking.

UCLA compiled the AC steady state flow rates from experiment (please see the table on next page). The air flow rate at the tank entrance is first adjusted by the torque (BMEP), and the adjusted flow rate is in the second to last column. The adjustment is a simple scaling of the air flow rate, using the ratio between the requested torque and the achieved torque.

The adjusted air flow rate is compared with the simulated air flow rate and the results are in the last column. So the highest percentage is 79.45%, the lowest is 18.84% and the average is 44.53%. The simulated air flow rate tables are scaled using these three numbers to estimate the air flow rate of the experiment for the best case, the worst case, and the average case.

The flow rate tables are then used to do the vehicle driving simulation. Note AM flow rates are unavailable and are not scaled. The results are in the following table for three different driving schedules:

	79.45% AC air flow (best)	18.84% AC air flow (worst)	44.53% AC air flow (average)	Simulation (Phase II)
NY Composite	14.71%	7.17%	10.24%	18%
WHM	8.72%	4.67%	6.54%	10%
WVU Suburban	7.96%	4.09%	6.09%	9%

N

Note that the improvement numbers are still from vehicle driving simulation.

The difference is that the air flow rates from the experiment are incorporated. Compared to the Phase II simulation results, the improvements are lower even for the best case we had from the experiment.

The estimation is very rough, but it uses a lot more information from the experiment and involves real driving cycle simulation.

7 Presentation and Publication

Publications

1. “Demonstration of Air-Power-Assist Engine Technology for clean combustion and direct energy recovery in heavy duty application”, ***Phase III Quarterly Reports***, ***January, July and October 2007.***

2. Kang, H., Tai, C., Smith, E., Wang, X., Tsao, T-C., Blumberg, P.N., and Stewart, J., “Demonstration of Air-Power-Assist Engine Technology for clean combustion and direct energy recovery in heavy duty application”, ***SAE Technical Paper,2008-01-1197, 2008***.

3. Wang, X., Tsao, T-C., Kang, H., Tai, C., and Blumberg, P.N., “Modeling of Compressed Air Hybrid Operation for a Heavy Duty Diesel Engine”, ***ASME Spring Technical Paper, ICES2008-1679, 2008.***

Presentations

1. Kang, H., “APA project technical review”, Local Internal Review Presentation, ***Hagerstown, MD. January and September 2007.***

2. Tai, C., “APA project technical review” Presentation for DOE merit review, ***Washington D.C. June, 2007***.

3. Kang, H., “Demonstration of Air-Power-Assist Engine Technology for clean combustion and direct energy recovery in heavy duty application”, ***Aug. 14th DEER Conference, Detroit, 2007***.

8 Acknowledgement

I would like to give appreciation to the following people for their great efforts and time to complete APA project successfully.

VPTNA: Dr. Chun Tai, Mr. Edward Smith, Mr. Doug Stine

UCLA: Dr. T-C Tao, Mr. Xioayong Wang

Sturman Ind. : Mr. Jeff Stewart and Mr. Lane Christenesen

Consultant: Dr. Paul N. Blumberg

U.S Department of Energy (DOE): Mr. Samuel Taylor